Design of asymmetric DNAzymes for dynamic control of nanoparticle aggregation states in response to chemical stimuli†

Juewen Liu and Yi Lu*

Received 24th April 2006, Accepted 9th June 2006
First published as an Advance Article on the web 3rd July 2006
DOI: 10.1039/b605799c

Dynamic control of nanomaterial assembly states in response to chemical stimuli is critical in making multi-component materials with interesting properties. Previous work has shown that a Pb^{2+}-specific DNAzyme allowed dynamic control of gold nanoparticle aggregation states in response to Pb^{2+}, and the resulting color change from blue aggregates to red dispersed particles can be used as a convenient way of sensing Pb^{2+}. However, a small piece of DNA (called invasive DNA) and low ionic strength (~30 mM) were required for the process, limiting the scope of application in assembly and sensing. To overcome this limitation, a series of asymmetric DNAzymes, in which one of the two substrate binding regions is longer than the other, has been developed. With such a system, we demonstrated Pb^{2+}-induced disassembly of gold nanoparticle aggregates and corresponding color change at room temperature without the need for invasive DNA, while also making the system more tolerant to ionic strength (33–100 mM). The optimal lengths of the long and short arms were determined to be 14 and 5 base pairs, respectively. In nanoparticle aggregates, the activity of the DNAzyme increased with decreasing ionic strength of the reaction buffer. This simpler and more versatile system allows even better dynamic control of nanoparticle aggregation states in response to chemical stimuli such as Pb^{2+}, and can be used in a wider range of applications for colorimetric sensing of metal ions.

Introduction

Recent progress in nanoscale science and engineering has resulted in a number of new nanomaterials with interesting properties.[1–5] To realize its true potential for practical applications such as in electronic and photonic industries, one needs to control the assembly processes not only thermodynamically, such as through variation of external variables including temperature, pH and concentration of starting materials, but also dynamically, such as controlling the initiation, growth and termination of assembly processes in response to a particular chemical signal under thermodynamic equilibrium conditions. In this regard, biomaterials such as bones and shells set excellent examples, where all the processes occur under ambient conditions in response to internal chemical stimuli that signal the need for making the materials. Biology-inspired studies are important for advancing nanoscale science and technology. One such inspiration is the use of nucleic acids for dynamic control of a number of biological processes including protein synthesis and biomaterials assembly.

Long considered to be only in the life sciences domain, nucleic acids have been used as versatile templates and building blocks in materials science for over a quarter of a century.[6–11] Inspired by biology and recent developments in materials science, we are interested in using nucleic acids for dynamic control of nanomaterial assembly.[12–17] A particularly interesting class of nucleic acids is DNAzymes, *i.e.*, DNA molecules with enzymatic activities (also called catalytic DNA, DNA enzymes, or deoxyribozymes elsewhere).[18–25] A DNAzyme is a special class of DNA chain that usually contains both double and single stranded regions that fold into a specific three-dimensional structure like globular proteins, in order to perform a catalytic function. Because they are made of DNA, DNAzymes have the advantage of being highly stable and cost effective compared to protein- or RNA-based enzymes, and thus are readily applicable for materials science and engineering. DNAzymes that are specifically activated by a particular chemical species such as a metal ion can be isolated through a combinatorial biology process called *in vitro* selection, which qualifies DNAzymes as an excellent choice for dynamic control of nanomaterials assembly.[21,26,27] Importantly, the metal binding affinity and specificity can be tuned. For example, the 8–17 DNAzyme (Fig. 1a) contains a substrate strand (17DS) and an enzyme strand (17E).[28–32] The DNAzyme catalyzes cleavage of 17DS into two fragments at the rA (ribo-adenosine) position only in the presence of Pb^{2+} (Fig. 1b).

Using the Pb^{2+}-specific DNAzyme, we have demonstrated dynamic control of gold nanoparticle aggregation states in response to Pb^{2+} as an internal stimulus.[12] To allow the DNAzyme to assemble nanoparticles, the substrate strand was extended on both ends with the extended parts being complementary to the DNA attached to the nanoparticles. Therefore, the extended substrate, the enzyme, and nanoparticles can form an aggregated structure, appearing blue due to the surface plasmon effect. Addition of Pb^{2+} resulted in specific cleavage of the substrate strand, preventing aggregation, and resulting in individual red-colored gold nanoparticles. Therefore, this process can be used for convenient colorimetric Pb^{2+} sensing. Initially, the nanoparticles were aligned in a head-to-tail manner (Fig. 1c), such that only one set of nanoparticles was needed. Despite the initial success, further improvement of the process was desirable, as the process required

Department of Chemistry, University of Illinois at Urbana–Champaign, Urbana, IL, 61801, USA. E-mail: yi-lu@uiuc.edu; Fax: +1 217-3332685; Tel: +1 217 3332619

† This paper was published as part of a themed issue on DNA-Based Nano-Architectures and Nano-Machines.

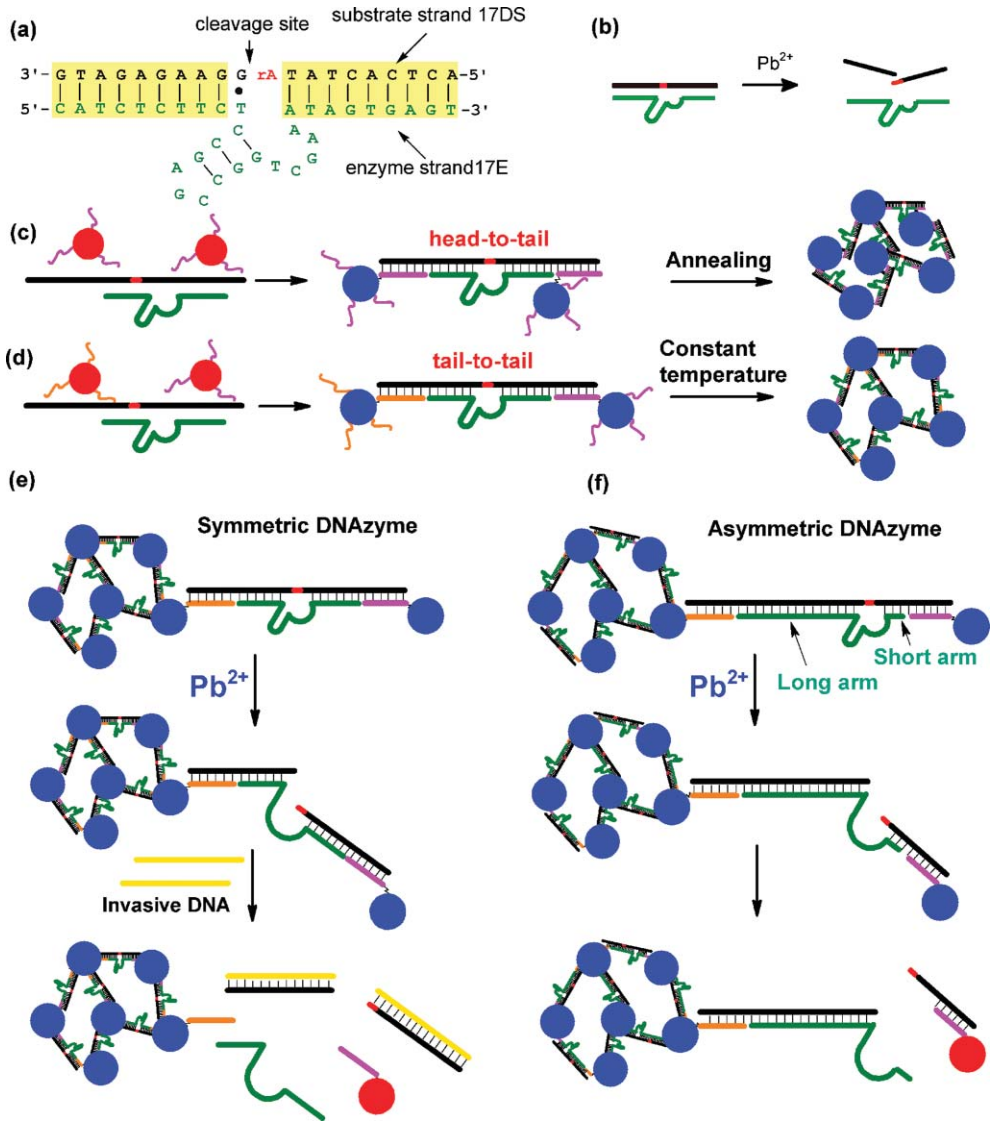

Fig. 1 (a) Secondary structure of the Pb^{2+}-specific 8–17 DNAzyme. (b) Cleavage of the substrate in the presence of Pb^{2+}. The substrate was extended on both ends to bind nanoparticles. (c) Formation of head-to-tail aligned nanoparticle aggregates linked by the DNAzyme. (d) Formation of tail-to-tail aligned aggregates. (e) Invasive DNA-aided disassembly of nanoparticle aggregates linked by the symmetric DNAzyme. (f) Disassembly of nanoparticle aggregates linked by asymmetric DNAzymes.

a two hour annealing process from 50 °C to room temperature.[12] To improve the process to more closely mimic those in biology (*i.e.*, ambient conditions), we have carried out detailed studies on the system, which suggested that by aligning the nanoparticles in a tail-to-tail manner (Fig. 1d), the nanoparticles could aggregate at a constant temperature. When large nanoparticles (*i.e.*, 42 nm in diameter instead of 13 nm) were used, the aggregation process was close to completion in ~5 minutes.[13]

After demonstrating Pb^{2+}-directed assembly of gold nanoparticles, the next challenge was to study the reverse process: Pb^{2+}-induced disassembly of DNAzyme-linked nanoparticle aggregates. In such an aggregate, the DNAzyme was sandwiched between two nanoparticles.[15] In contrast, most known systems of immobilized protein and RNA-based enzymes have only a single anchoring point on the enzyme, resulting in a large degree of freedom, and thus similar activity to the free enzyme in the solution phase.[33,34] By confining the DNAzyme to a compact network structure containing thousands of nanoparticles, the activity of the DNAzyme was challenged. For example, the DNAzyme was inactive when the nanoparticles were aligned in a head-to-tail manner. Activity was only observed when the nanoparticles were arranged tail-to-tail.[15]

Upon addition of Pb^{2+} to the tail-to-tail aligned aggregates, the substrate cleavage reaction was initiated. There was, however, no observable blue-to-red color change. This was attributed to the remaining linkage between the enzyme strand and the two cleaved substrate fragments, resulting in no release of nanoparticles (Fig. 1e, the first step).[15] To facilitate release of nanoparticles, the following two methods were employed at the same time. First, the NaCl concentration was decreased from 300 mM to 30 mM to make the aggregates in a metastable state. Even lower NaCl concentrations led to aggregate instability and thus could not be pursued. Second, two short pieces of DNA (called invasive DNA) complementary to the cleaved substrate fragments were

added (Fig. 1e, the second step). If the NaCl concentration was high (*i.e.*, 100 mM), disassembly was not observed after a day, even with invasive DNA and Pb^{2+}.[15] The need for very low ionic strength and invasive DNA makes disassembly and colorimetric sensing less practical. Herein, we describe the development of a new method of using asymmetric DNAzymes to facilitate the release of nanoparticles after addition of Pb^{2+}, which can be carried out in the *absence* of invasive DNA and in relatively high salt buffers. This simpler and more versatile system allows even better dynamic control of nanoparticle aggregation states in response to chemical stimuli such as Pb^{2+} and can be used in a wider range of applications for colorimetric sensing of metal ions. In addition, the asymmetric DNAzyme system demonstrated here offers an ideal platform to study interactions between biopolymers with inorganic nanoparticles in a systematic manner.

Results and discussion

System design

The DNAzyme used in the original system (17E) forms symmetrical Watson–Crick base pairs with the substrate strand (17DS), with 9 base pairs on each side (Fig. 1a). If the DNAzyme is free in solution, binding of Pb^{2+} causes cleavage of 17DS and dissociation of the cleaved fragments from the enzyme strand, which is the basis of designing fluorescent Pb^{2+} sensors with the DNAzyme.[35,36] In nanoparticle aggregates, however, the DNAzyme is immobilized on both ends in a large nanoparticle network structure, and the motion of the DNAzyme is confined. After cleavage, it is not clear whether the substrate fragments are transiently dissociated from the enzyme or not. Even if the dissociation process does occur, they have a high chance of re-associating because the enzyme and substrate fragments are still positioned closely together. This could explain why nanoparticle aggregates were maintained, even in the presence of Pb^{2+}.

The substrate is associated with the enzyme through two base paired arms (Fig. 1a, in yellow). The lengths of the two arms can vary, as long as the base pairing interactions remain strong enough to hold the substrate and enzyme together. By shortening one arm and elongating the other, the dissociation of the shortened substrate piece after the cleavage reaction should be facilitated, while still maintaining aggregate stability before cleavage. The resulting new DNAzymes have two substrate binding arms of different lengths, and are therefore called asymmetric DNAzymes. In comparison to the original symmetrical DNAzyme, the Pb^{2+}-induced disassembly of asymmetric DNAzyme-linked aggregates should be spontaneous and less difficult. This process is summarized in Fig. 1f. To identify the optimal construct of an asymmetric DNAzyme, the lengths of the two substrate binding arms need to be optimized.

Optimization of the short arm

To optimize the lengths of the two arms, a matrix of samples is usually needed to cover all the possibilities, especially if the two arms are similar in length and some synergy exists between the two arms. In this particular case, however, the two arms were designed to be drastically different in length. Therefore, a small change in the length of one arm should have minimal effect on the performance of the other, and the two arms can be optimized independently. Because it is the short arm that governs the rate of dissociation after cleavage, its length was optimized first. It is known that the G·T wobble pair (Fig. 1a) downstream of the cleavage site is important for the activity of the DNAzyme.[28,30,37] To minimize perturbations on the performance of the DNAzyme, the arm containing the wobble pair was extended while the other arm was shortened. Four DNAzymes were prepared with the same substrate strand that was shortened on the short arm by 3 nucleotides and extended on the long arm by 5 nucleotides. This new substrate was therefore named (−3)Sub_{Au}(5). Accordingly, four enzyme strands were prepared with the corresponding long arm extended by 5 nucleotides on the basis of 17E, and the short arm decreased by 3, 4, 5, or 6 nucleotides (Fig. 2a). To ensure that such extensions and truncations do not perturb the

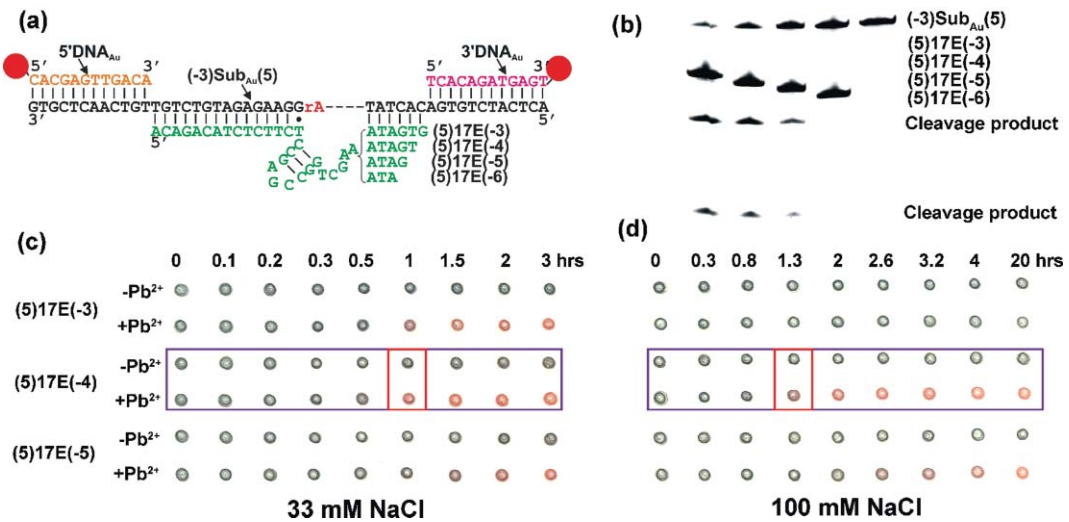

Fig. 2 Optimization of the short arm of the asymmetric DNAzyme. (a) Secondary structures of four asymmetric DNAzymes. The short arm of the asymmetric DNAzyme is varied from 3 to 6 base pairs. (b) Assay of the asymmetric DNAzyme with different short arm lengths. Monitoring Pb^{2+}-induced color change of asymmetric DNAzyme-assembled nanoparticle aggregates with (c) 33 mM NaCl or (d) 100 mM NaCl.

enzymatic activities, a solution phase assay of the four DNAzyme constructs was performed. The DNAzymes were incubated with 5 μM Pb^{2+} for 2 minutes and the reactions were assayed by gel electrophoresis and ethidium bromide staining. The results are presented in Fig. 2b. The substrate was the longest strand and therefore should have the lowest mobility, appearing at the top of the gel. The lengths of the four enzyme strands differ from each other by one nucleotide, and indeed four bands at different positions were observed. The assignment of each band was also provided in the figure. The lowest two bands were assigned to be the cleavage products.

As can be observed from the gel, the intensity of the cleavage product bands decreased with decreasing length of the short arm. The DNAzyme with only 3 base pairs on the short arm did not give observable cleavage products and was not used in further optimizations. This result is consistent with previous studies carried out on another DNAzyme, whose activity can be inhibited if the binding arm is too short.[38] To further investigate the best candidate among the three remaining DNAzymes, nanoparticles were assembled by the three DNAzymes as shown in Fig. 1f. After addition of Pb^{2+}, the kinetics of color change was monitored by spotting aliquots of nanoparticles at designated time points. As a control, aggregates with no added Pb^{2+} were also spotted at the same time points. The study was performed at two NaCl concentrations: 33 mM (Fig. 2c) and 100 mM (Fig. 2d). With increasing time, a color transition from blue to red was observed in most samples in the presence of Pb^{2+}. Since all controls without Pb^{2+} remained blue, the observed color changes were attributable to Pb^{2+}-induced cleavage instead of artifacts. The time points at which the first red spot emerged are highlighted by red boxes. The (5)17E(−4) assembled aggregates gave the fastest color change from blue to red at both ionic strength conditions (highlighted in purple boxes). As analyzed in Fig. 1f, the observed color change should be affected by both DNAzyme cleavage and subsequent nanoparticle release. This hypothesis is supported by the data in Fig. 2c and 2d. The (5)17E(−4) had higher activity compared to (5)17E(−5), while the (5)17E(−4) had a higher rate of nanoparticle release than (5)17E(−3). As a compromise between the two factors (cleavage activity and nanoparticle release), the enzyme with 4 nucleotides removed from the short arm (5 base pairs remaining) is optimal for Pb^{2+}-induced disassembly.

When the performance of each enzyme was compared at the two NaCl concentrations, the (5)17E(−3) enzyme displayed a color change in 33 mM NaCl, but not in 100 mM NaCl, suggesting that the release of the short arm fragment with 6 base pairs was inhibited in the presence of 100 mM NaCl. For the other two enzymes, the rates of color change were also faster in the low salt buffer. These results further supported the idea that the DNAzyme was active in nanoparticle aggregates, and the release of nanoparticles after cleavage may be inhibited.

Optimization of the long arm

After determining the optimal length of the short arm to be 5 base pairs, three DNAzymes with the long arm extended by 2, 5, and 10 base pairs were prepared to optimize the long arm (Fig. 3a). The substrate strand for the study was (−4)Sub_{Au}(10). Because the kinetics of disassembly is mostly governed by the length of the short arm, varying the length of the long arm may only have very small effects. Therefore, biochemical assays were performed to optimize the long arm. The substrate was labeled with ^{32}P on the 5′-end, so that the cleavage activities could be followed by gel electrophoresis. A small fraction of the labeled substrate was mixed with unlabeled substrate to assemble gold nanoparticle aggregates. After separating the aggregates from free nanoparticles and DNAzymes, Pb^{2+} was added to the aggregates to initiate the cleavage reaction, and a small aliquot of aggregates was taken out and quenched with a stop buffer at designated time points. Finally, the aggregates in each aliquot were disassembled by heating to release the cleaved and uncleaved substrates for gel electrophoresis analysis. The (2)17E(−4) and (5)17E(−4) enzymes were very active, as more than half of the substrate was cleaved in the first 30 seconds (Fig. 3b). Further increase of the long arm decreased the activity. It is not clear what caused this decrease however. For all three test systems, the final cleavage after

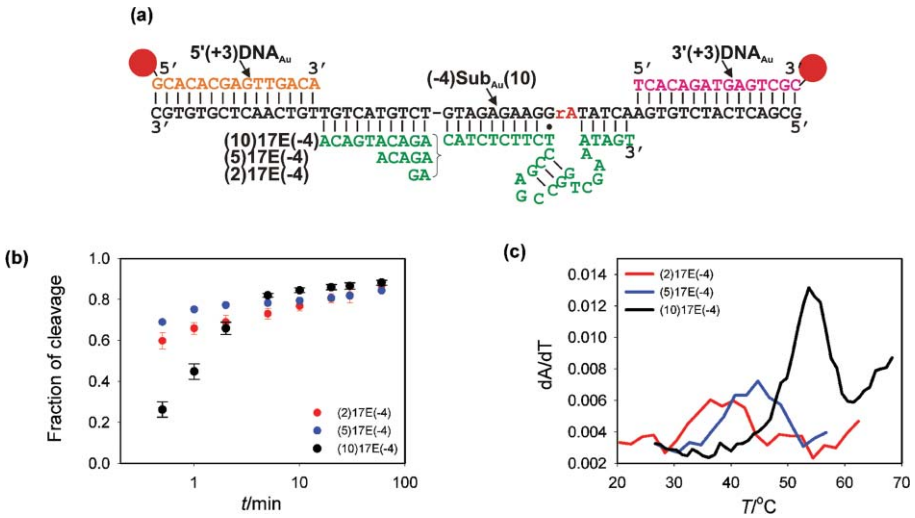

Fig. 3 Optimization of the long arm of the asymmetric DNAzyme. (a) Three DNAzymes with 11, 14, and 19 base pairs on the long arm were tested. (b) Activity assays with the three DNAzymes embedded in nanoparticle aggregates. (c) First derivative of melting curves of the three DNAzymes in solution phase.

one hour reached ~80%. The original 17E enzyme (9 base pairs on the long arm) had a maximal cleavage of only 60%,[15] which could be attributed to the dissociation of the enzyme from the substrate. Therefore, introducing a long binding arm can increase the stability of the substrate/enzyme complex even though the other arm is shortened. Overall, elongating the long arm by 5 nucleotides offered the highest activity. Because the optimal long arm has been used to optimize the short arm, no further cross-optimizations were performed.

Melting curves of the three DNAzyme complexes in solution (not in nanoparticle aggregates) were also measured, and the first derivatives of the melting curves are shown in Fig. 3c. The two DNAzymes with 2 and 5 base pairs extended on the long arm did not show a well-defined melting transition, and broad melting processes were observed. The 10 base pair extended DNAzyme showed a relatively sharp transition, because its percentage of base paired nucleotides was the highest among the three. The melting temperatures of the three DNAzyme complexes were around 35, 45, and 53 °C, respectively. Higher melting temperatures should favor sensing applications, as the sensors can be used in a wider temperature range.

The effect of ionic strength

With the long and short arms of the asymmetric DNAzyme optimized, the effect of ionic strength on DNAzyme activity was also studied to pursue the best condition for disassembly. The (10)17E(−4) enzyme and the corresponding substrate shown in Fig. 3a were used for these studies. First, the kinetics of cleavage in aggregates dispersed in different NaCl concentrations were compared. As shown in Fig. 4a, the cleavage reaction was slower in high salt buffers. We hypothesize that the rate of cleavage should be the fastest at the outer layers of an aggregate, because DNAzymes in the inner layers could be in a more constrained state and thus display a lower activity. With high salt, the release of nanoparticles was slower. Indeed, with 300 mM NaCl, no color change was observed in the one hour reaction process, even though over 90% of the linking substrates were cleaved. An alternative explanation could be that the DNAzyme activity was slower at higher NaCl conditions. To test this, solution phase single turnover assays were performed at various NaCl concentrations, and the results are shown in Fig. 4b. The three rates were similar, with the reaction in 200 mM NaCl being the fastest. Therefore, high salt inhibition of DNAzyme activity was not the main cause of slower color change; instead, the main factor is proposed to be inhibition of disassembly at high salting conditions, which can slow the cleavage of the embedded DNAzymes. Therefore, lower NaCl buffers offered faster rates of cleavage in aggregates and also faster rates of color change.

Conclusions

By combining inorganic nanoparticles with biopolymers, new materials with novel properties and applications may be obtained. Nanoparticles and biopolymers have comparable dimensions. Therefore, subtle changes in each component may drastically affect the performance of the whole system. As demonstrated in this paper, a single nucleotide increase in DNA length can inhibit the disassembly of a whole aggregate. The asymmetric DNAzyme-linked nanostructures have provided us with a useful system to systematically study the interactions between a biocatalyst and nanoparticles. The knowledge learned from such studies will deepen the understanding of both components and help in the design of better sensors.

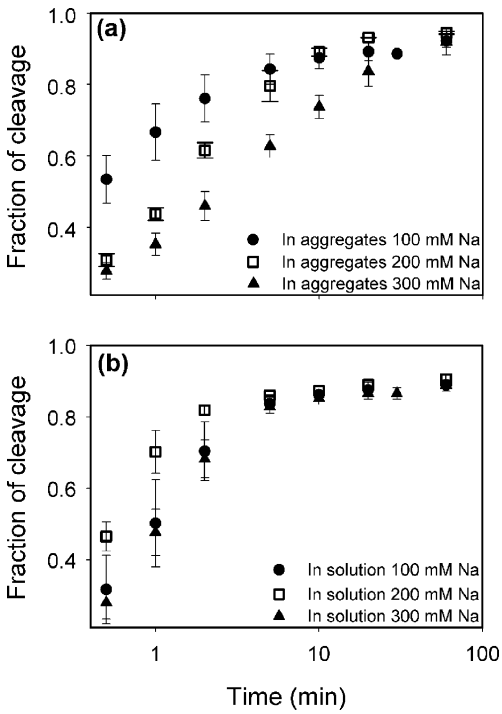

Fig. 4 Cleavage kinetics at various NaCl conditions of DNAzymes (a) in the assembled state and (b) in solution.

Experimental

Materials

All DNA samples were purchased from Integrated DNA Technologies Inc. (Coralville, IA). The names and DNA sequences are listed in Table 1. The substrates and enzymes of the DNAzyme were purified by HPLC or polyacrylamide gel electrophoresis. Thiol-modified DNA molecules were purified by standard desalting. The synthesis of gold nanoparticles (13 nm diameter), and the attachment of thiol-modified DNA to gold nanoparticles are described in detail elsewhere.[15,39]

Biochemical assays monitored by ethidium bromide staining

Five microcentrifuge tubes were prepared. Each tube contained 4 μM of (−3)Sub_{Au}(5) substrate, 100 mM NaCl, and 25 mM Tris acetate, pH 8.2. Nothing else was added to the first tube, 5 μM of the four enzymes (5)17E(−3), (5)17E(−4), (5)17E(−5), or (5)17E(−6) were added to the remaining four tubes. After annealing the DNA in each tube, a final concentration of 5 μM of $Pb(OAc)_2$ was added to initiate the cleavage reaction. After 2 min, a stop buffer containing 90% formamide and 1 mM EDTA was added to quench the reaction. The solution in the tube was loaded

Table 1 Names and sequences of DNA used in this study

Name	Sequence (listed from the 5′- to the 3′-end)
(−3)Sub_{Au}(5)	ACTCATCTGTGACACTATrAGGAAGAGATGTCTGTTGTCAACTCGTG
(−4)Sub_{Au}(10)	GCGACTCATCTGTGAACTATrAGGAAGAGATGTCTGTACTGTTGTCAACTCGTGTGC
(5)17E(−3)	ACAGACATCTCTTCTCCGAGCCGGTCGAAATAGTG
(5)17E(−4)	ACAGACATCTCTTCTCCGAGCCGGTCGAAATAGT
(5)17E(−5)	ACAGACATCTCTTCTCCGAGCCGGTCGAAATAG
(5)17E(−6)	ACAGACATCTCTTCTCCGAGCCGGTCGAAATA
(2)17E(−4)	GACATCTCTTCTCCGAGCCGGTCGAAATAGT
(10)17E(−4)	ACAGTACAGACATCTCTTCTCCGAGCCGGTCGAAATAGT
3′DNA_{Au}	TCACAGATGAGT-$(CH_2)_3$-S-Au nanoparticle
5′DNA_{Au}	Au nanoparticle-S-$(CH_2)_6$-CACGAGTTGACA
3′(+3)DNA_{Au}	TCACAGATGAGTCGC-$(CH_2)_3$-S-Au nanoparticle
5′(+3)DNA_{Au}	Au nanoparticle-S-$(CH_2)_6$-GCACACGAGTTGACA

onto a 20% denaturing PAGE gel for analysis, and the gel was stained by 20 μL of ethidium bromide in 70 mL water for 20 min. The gel was imaged by exciting at 532 nm and the emission filter was set at 580 nm on a FLA-3000 fluorescence imager.

Preparation of gold nanoparticle aggregates

To prepare aggregates, a solution was prepared containing 6 nM 3′DNA_{Au}, 6 nM 5′DNA_{Au}, 400 nM enzyme, 100 nM substrate, 300 mM NaCl and 25 mM Tris acetate buffer, pH 8.2. The final extinction at 522 nm was ~2.2. The mixture was warmed to 60 °C for 3 min and allowed to cool slowly to room temperature over 4 h in a water bath. After brief centrifugation, dark purple nanoparticle aggregates precipitated to the bottom. The supernatant was removed and the aggregates were washed three times with a buffer containing 300 mM NaCl and 25 mM Tris acetate, pH 8.2, and were finally suspended in the same buffer.

Biochemical assay for DNAzyme embedded in nanoparticle aggregates

^{32}P-Labeled aggregates were added to a solution with 30 μM Pb^{2+}, designated NaCl concentrations (*i.e.* 100, 200, or 300 mM), and 25 mM Tris acetate, pH 8.2. Aliquots were taken out at designated time points and quenched in a solution containing 8 M urea and 200 mM EDTA. The quenched aliquots were heated at 60 °C to fully release substrate strands from aggregates and then loaded onto a 20% denaturing polyacrylamide gel. ^{32}P-Labeling and procedures for single-turnover solution phase activity assays were the same as reported elsewhere.[30,37] To monitor the color change by spotting on an alumina TLC plate, aggregates linked by various enzyme strands and (5)Sub_{Au}(−3) (not ^{32}P-labeled) were suspended in a solution containing 100 mM or 33 mM NaCl, 25 mM Tris acetate, pH 8.2. Either no Pb^{2+} or 10 μM Pb^{2+} was added, and aliquots were taken out at designated time points for spotting onto a TLC plate.

Acknowledgements

This material is based upon work supported by the Department of Energy (DEFG02-01-ER63179), the US Army Research Laboratory and the US Army Research Office under grant number DAAD19-03-1-0227, and by the National Science Foundation through a Nanoscale Science and Engineering Center grant (DMR-0117792).

References

1 J. J. Storhoff and C. A. Mirkin, *Chem. Rev.*, 1999, **99**, 1849–1862.
2 *WTEC Panel on Nanostructure Science and Technology—R & D Status and Trends in Nanoparticles, Nanostructured Materials, and Nanodevices*, ed. R. W. Siegel, E. Hu and M. C. Roco, Kluwer Academic Publishers, Boston, 1999.
3 C. M. Niemeyer, *Angew. Chem., Int. Ed.*, 2001, **40**, 4128–4158.
4 E. Katz and I. Willner, *Angew. Chem., Int. Ed.*, 2004, **43**, 6042–6108.
5 Y. Yin and A. P. Alivisatos, *Nature*, 2005, **437**, 664–670.
6 N. C. Seeman, *Nature*, 2003, **421**, 427–431.
7 J. Sharma, R. Chhabra, Y. Liu, Y. Ke and H. Yan, *Angew. Chem., Int. Ed.*, 2006, **45**, 730.
8 H. Yan, S. H. Park, G. Finkelstein, J. H. Reif and T. H. LaBean, *Science*, 2003, **301**, 1882–1884.
9 Y. Ke, Y. Liu, J. Zhang and H. Yan, *J. Am. Chem. Soc.*, 2006, **128**, 4414.
10 Y. Liu, Y. Ke and H. Yan, *J. Am. Chem. Soc.*, 2005, **127**, 17140.
11 Z. Deng, Y. Tian, S.-H. Lee, A. E. Ribbe and C. Mao, *Angew. Chem., Int. Ed.*, 2005, **44**, 3582–3585.
12 J. Liu and Y. Lu, *J. Am. Chem. Soc.*, 2003, **125**, 6642–6643.
13 J. Liu and Y. Lu, *J. Am. Chem. Soc.*, 2004, **126**, 12298–12305.
14 J. Liu and Y. Lu, *Chem. Mater.*, 2004, **16**, 3231–3238.
15 J. Liu and Y. Lu, *J. Am. Chem. Soc.*, 2005, **127**, 12677–12683.
16 J. Liu, D. P. Wernette and Y. Lu, *Angew. Chem., Int. Ed.*, 2005, **44**, 7290–7293.
17 J. Liu and Y. Lu, *Angew. Chem., Int. Ed.*, 2006, **45**, 90.
18 R. R. Breaker, *Nat. Biotechnol.*, 1997, **15**, 427–431.
19 R. R. Breaker, *Curr. Opin. Chem. Biol.*, 1997, **1**, 26–31.
20 D. Sen and C. R. Geyer, *Curr. Opin. Chem. Biol.*, 1998, **2**, 680–687.
21 Y. Lu, *Chem. Eur. J.*, 2002, **8**, 4588–4596.
22 G. F. Joyce, *Annu. Rev. Biochem.*, 2004, **73**, 791–836.
23 J. C. Achenbach, W. Chiuman, R. P. G. Cruz and Y. Li, *Curr. Pharm. Biotechnol.*, 2004, **5**, 312–336.
24 A. Peracchi, M. Bonaccio and M. Clerici, *J. Mol. Biol.*, 2005, **352**, 783–794.
25 S. K. Silverman, *Nucleic Acids Res.*, 2005, **33**, 6151–6163.
26 P. Bruesehoff, J., J. Li, A. J. Augustine and Y. Lu, *Comb. Chem. High Throughput Screening*, 2002, **5**, 327–335.
27 Y. Lu, J. Liu, J. Li, P. J. Bruesehoff, C. M. B. Pavot and A. K. Brown, *Biosens. Bioelectron.*, 2003, **18**, 529–540.
28 S. W. Santoro and G. F. Joyce, *Proc. Natl. Acad. Sci. U. S. A.*, 1997, **94**, 4262–4266.
29 D. Faulhammer and M. Famulok, *Angew. Chem., Int. Ed. Engl.*, 1996, **35**, 2837–2841.
30 J. Li, W. Zheng, A. H. Kwon and Y. Lu, *Nucleic Acids Res.*, 2000, **28**, 481–488.
31 A. Peracchi, *J. Biol. Chem.*, 2000, **275**, 11693–11697.
32 R. P. G. Cruz, J. B. Withers and Y. Li, *Chem. Biol.*, 2004, **11**, 57–67.

33 A. A. Vertegel, R. W. Siegel and J. S. Dordick, *Langmuir*, 2004, **20**, 6800.
34 C. B. Swearingen, D. P. Wernette, D. M. Cropek, Y. Lu, J. V. Sweedler and P. W. Bohn, *Anal. Chem.*, 2005, **77**, 442–448.
35 J. Li and Y. Lu, *J. Am. Chem. Soc.*, 2000, **122**, 10466–10467.
36 J. Liu and Y. Lu, *Anal. Chem.*, 2003, **75**, 6666–6672.
37 A. K. Brown, J. Li, C. M. B. Pavot and Y. Lu, *Biochemistry*, 2003, **42**, 7152–7161.
38 S. W. Santoro and G. F. Joyce, *Biochemistry*, 1998, **37**, 13330–13342.
39 J. J. Storhoff, R. Elghanian, R. C. Mucic, C. A. Mirkin and R. L. Letsinger, *J. Am. Chem. Soc.*, 1998, **120**, 1959–1964.